THE JOURNAL OF BIOLOGICAL CHEMISTRY
Vol. 276, No. 13, Issue of March 30, pp. 10514–10523, 2001

*Printed in U.S.A.*

# Regulation of the Processing of Glucose-6-phosphate Dehydrogenase mRNA by Nutritional Status*

Received for publication, November 21, 2000, and in revised form, December 19, 2000
Published, JBC Papers in Press, December 21, 2000, DOI 10.1074/jbc.M010535200

**Batoul Amir-Ahmady and Lisa M. Salati‡**

*From the Department of Biochemistry, West Virginia University, Morgantown, West Virginia 26506*

**Expression of glucose-6-phosphate dehydrogenase (G6PD) gene during starvation and refeeding is regulated by a posttranscriptional mechanism occurring in the nucleus. The amount of G6PD mRNA at different stages of processing was measured in RNA isolated from the nuclear matrix fraction of mouse liver. This nuclear fraction contains nascent transcripts and RNA undergoing processing. Using a ribonuclease protection assay with probes that cross an exon-intron boundary in the G6PD transcript, the abundance of mRNAs that contain the intron (unspliced) and without the intron (spliced) was measured. Refeeding resulted in 6- and 8-fold increases in abundance of G6PD unspliced and spliced RNA, respectively, in the nuclear matrix fraction. However, the amount of G6PD unspliced RNA was at most 15% of the amount of spliced RNA. During refeeding, G6PD spliced RNA accumulated at a rate significantly greater than unspliced RNA. Further, the amount of partially spliced RNA exceeded the amount of unspliced RNA indicating that the enhanced accumulation occurs early in processing. Starvation and refeeding did not regulate either the rate of polyadenylation or the length of the poly(A) tail. Thus, the G6PD gene is regulated during refeeding by enhanced efficiency of splicing of its RNA, and this processing protects the mRNA from decay, a novel mechanism for nutritional regulation of gene expression.**

Glucose-6-phosphate dehydrogenase (G6PD,[1] EC 1.1.1.49) is the rate-limiting enzyme of the pentose phosphate pathway. All cells contain G6PD activity; however, nutritional and hormonal factors only regulate the expression of the enzyme in liver and adipose tissue (1–3). Regulation of G6PD activity in these tissues is because it plays a critical role in the *de novo* synthesis of fatty acids by providing 50–75% of the NADPH for the fatty acid synthase reaction (4). Thus, G6PD is a member of the lipogenic enzyme family. The activities of the lipogenic enzymes are coordinately regulated so that flux of substrate through the fatty acid biosynthetic pathway is high when animals consume a diet rich in carbohydrate and flux is decreased by starvation or the addition of polyunsaturated fat to the diet (reviewed in Ref. 5). However, the molecular mechanisms causing these changes in flux vary considerably between enzymes.

The enzymes of the fatty acid biosynthetic pathway are regulated at both transcriptional and posttranscriptional steps. Fatty acid synthase (6–8), acetyl-CoA carboxylase (9, 10), stearoyl-CoA desaturase (11), and ATP-citrate lyase (12) undergo large changes in their transcriptional rates in response to dietary manipulations. Regulation of malic enzyme expression during a chow to fat-free diet transition occurs by changes in mRNA stability in the cytoplasm (13). In addition, cytoplasmic mRNA stability is also involved in the regulation of stearoyl-CoA desaturase expression by fatty acids in yeast (14) and in adipocytes (15). Posttranscriptional regulation is the primary mechanism involved in the nutritional regulation of G6PD expression and the mechanism involved occurs entirely within the nucleus.

G6PD expression undergoes large changes in expression in the livers of starved and refed mice and rats (3, 16, 17). These nutritionally induced changes in G6PD activity are pretranslational (17–21). Despite the 12–15-fold increase in G6PD mRNA abundance in the refed mouse, the transcriptional activity of the gene is not changed (22). This increase in cytoplasmic G6PD mRNA due to refeeding is accompanied by an increase in the amount of G6PD precursor mRNA (pre-mRNA) in the nucleus implicating steps early in the processing pathway as a potentially regulated point (23). Further, the increases in the cytoplasmic pool of G6PD mRNA are preceded by changes in the amount of the nuclear pool indicating that nuclear transport of the mature mRNA is not regulated (23). Nutritional regulation of gene expression primarily at a nuclear posttranscriptional level is a novel observation for a lipogenic gene. G6PD is an excellent model to further study nuclear posttranscriptional regulation because of the absence of transcriptional changes, which confound the interpretation of results.

The steps involved in processing of nascent transcripts into mature mRNA appear to be organized in a dynamic manner within the nucleus. Both the transcription of an RNA and its processing are spatially linked within the nucleus, such that only the mature mRNA leaves the site of transcription. The insoluble portion of the nucleus, which is the material remaining after sequential extraction of cells with detergent, DNase I, and salt (24–26), contains the hyperphosphorylated form of the large subunit of RNA polymerase II, transcription factors, a subset of small nuclear ribonucleoprotein particles, serine/arginine-rich (SR) protein splicing factors, and pre-mRNA (27–34). The spatial link between transcription and processing appears to be facilitated by RNA polymerase II. Upon phosphorylation of the C-terminal domain of polymerase II, proteins involved in capping, splicing and polyadenylation bind

* This work was supported by Grant DK46897 from the National Institutes of Health. The costs of publication of this article were defrayed in part by the payment of page charges. This article must therefore be hereby marked "*advertisement*" in accordance with 18 U.S.C. Section 1734 solely to indicate this fact.

‡ To whom correspondence should be addressed: Dept. of Biochemistry, West Virginia University, Health Sciences Center, P. O. Box 9142, Morgantown, WV 26506. Tel.: 304-293-7759; Fax: 304-293-6846; E-mail: lsalati@hsc.wvu.edu.

[1] The abbreviations used used: G6PD, glucose-6-phosphate dehydrogenase; pre-mRNA, precursor mRNA; NuMA, nuclear mitotic apparatus protein; SR, serine and arginine-rich; SRm160, SR-related matrix protein of approximately 160 kDa; CAT, chloramphenicol acetyltransferase; PAGE, polyacrylamide gel electrophoresis; mAb, monoclonal antibody; PCR, polymerase chain reaction; RSB, reticulocyte suspension buffer; PBS, phosphate-buffered saline; nt, nucleotide(s); bp, base pair(s); UTR, untranslated region.

to this domain and are thought to be transported to their site of action during the elongation process (35, 36). RNA that is not correctly processed does not leave the site of transcription and is degraded (37). Thus, the entry of a nascent transcript into the processing pathway and its efficient maturation are potential control points in the regulation of gene expression.

In this report, we present new results that nutritional regulation of G6PD expression occurs by changes in the efficiency of G6PD pre-mRNA splicing. We have explored this mechanism for regulation by measuring the amount of G6PD RNA that is undergoing processing in the livers of mice during starvation and refeeding a high carbohydrate diet. Refeeding a high carbohydrate diet enhanced the accumulation of G6PD mRNA in the processing pathway. The enhanced accumulation of G6PD mRNA was observed for RNA that was undergoing splicing regardless of the presence or absence of the poly(A) tail. Further, the length of the poly(A) tail was not regulated by nutritional changes. Thus, regulation by changes in the efficiency of pre-mRNA splicing represents an important mechanism for control of gene expression by nutritional status. Understanding the mechanisms by which nutrients alter nuclear posttranscriptional events will provide new information on the breadth of mechanisms involved in gene regulation.

## MATERIALS AND METHODS

*Cell Culture*—HepG2 cells (American Type Culture Collection, Rockville, MD) were grown in minimum essential medium (Life Technologies, Inc.) containing 110 mg/liter sodium pyruvate, penicillin (100 units/ml), streptomycin (100 $\mu$g/ml) (Life Technologies, Inc.), and 10% heat-inactivated fetal bovine serum (v/v; Life Technologies, Inc.) in a humidified atmosphere at 37 °C and 5% $CO_2$. MCF7 breast adenocarcinoma cells were a gift of Dr. Mike Miller (West Virginia University, Morgantown, WV) and were grown in Dulbecco's modified Eagle's medium supplemented with 10% fetal bovine serum and gentamicin (50 $\mu$g/ml). Rat hepatocytes were prepared as described previously (38). Lysates of MCF7 cells and rat hepatocytes were prepared by sonication of cells in phosphate-buffered saline (PBS).

*Animal Care*—Male C57BL/6 mice (NCI, Charles River Laboratory, Frederick, MD; 4 weeks of age) were adapted to a reverse-cycle room (light cycle 8 p.m. to 8 a.m.; dark cycle 8 a.m. to 8 p.m.) for 7 days while maintained on a standard chow diet (Harlan Teklad). Adaptation to a reverse light cycle permits the experiments to be done during typical work hours. Mice were switched to a fat-free diet with glucose as the carbohydrate source (PMI Feeds) supplemented with 1% (by weight) safflower oil as a source of essential fatty acids. Diet was prepared fresh daily, and the safflower oil was stored under $N_2$ to minimize oxidation. Mice received the high carbohydrate, low fat diet *ad libitum* for 7 days. On day 8, the food was removed for a 24-h starvation period followed by returning the diet for 24 h or for the times indicated in the figures.

*Cellular Fractionation*—Cellular fractionation was by a modification of the method of Leppard and Shenk (39). All steps except the DNase I digestion were preformed at −20 °C with 40% glycerol added to the buffers to prevent freezing (28). All solutions and glassware were treated to be RNase-free. Intactness of the RNA was monitored using Northern gels (data not shown); only intact RNA was used in subsequent steps. This modification was found to be superior to the use of vanadyl ribonucleoside complexes or a placental ribonuclease inhibitor in obtaining intact RNA.

Each mouse liver (or $2 \times 10^7$ cells in half the buffer volume) was homogenized in 6 ml isotonic buffer (150 mM NaCl, 10 mM Tris·Cl, pH 7.5, 1.5 mM $MgCl_2$, 1 mM phenylmethylsulfonyl fluoride, and 40% glycerol) with a motor driven Teflon pestle for 30 s. The cells were lysed by addition of 300 $\mu$l of 10% Nonidet P-40 (0.05%) and incubation at −20 °C for 5 min. The cytoplasmic fraction was collected following centrifugation at $2500 \times g$ for 10 min. The crude nuclear pellet was washed in 3 ml of isotonic buffer and then was resuspended in 3 ml of isotonic buffer containing Nonidet P-40 (0.5%) and sodium deoxycholate (0.25%). The mixture was vortexed and incubated at −20 °C for 5 min. The nuclear mixture was centrifuged as before, the supernatant was reserved, and was the nuclear membrane fraction. The remaining nuclear pellet was washed in 2 ml of reticulocyte suspension buffer (RSB; 10 mM NaCl, 10 mM Tris·Cl, pH 7.5, 4 mM $MgCl_2$, 1 mM phenylmethylsulfonyl fluoride, and 40% glycerol), pelleted as before, and the supernatant was added to the nuclear membrane fraction. The nuclear pellet was then resuspended in 500 $\mu$l of RSB (no glycerol) and incubated with RNase-free DNase I (1000 units, Life Technologies, Inc.) in the presence of 500 units of Prime RNase inhibitor (5Prime → 3Prime, Inc.) at 4 °C for 25 min (for Western analysis, ribonucleoside vanadyl complexes (5 mM; Sigma) were added instead of the protein based inhibitor). At the end of the DNase I digestion, glycerol (40%) was added and the mixture was centrifuged ($2500 \times g$, −20 °C, 15 min). The supernatant was reserved and was the nuclear soluble fraction. Nuclei were depleted of digested chromatin and associated proteins by addition of 2 ml of RSB and NaCl (1 M) and incubation for 10 min at −20 °C. The remaining nuclear material was pelleted as before, and the supernatant was added to the nuclear soluble fraction. The final pellet of insoluble nuclear material was reserved and is referred to here as the nuclear matrix (39).

*RNA Isolation*—RNA was isolated from the cytoplasm, nuclear membrane, and nuclear soluble fractions by addition of an equal volume of denaturing solution (8 M urea, 350 mM NaCl, 10 mM Tris·Cl, pH 7.5, 10 mM EDTA, 1% SDS) (39). An equal volume of phenol/chloroform (6:4) and 0.1 volume sodium acetate (2 M, pH 4.0) were added, and the mixture was vortexed and incubated on ice for 15 min. Following centrifugation to separate the layers, the aqueous phase from each fraction was removed and the RNA was precipitated by addition of equal volume of isopropanol. RNA from the nuclear matrix pellet was isolated by the method of Chomczynski and Sacchi (40).

*Nuclear RNA Isolation*—Nuclei were prepared by the citric acid protocol as described (23). RNA was isolated from the nuclear pellet by the method of Chomczynski and Sacchi (40).

*Electrophoresis and Western Blot Analysis*—Proteins in the cellular fractions (except nuclear matrix) were concentrated using a Centricon 30 (Amicon, Inc.). The protein concentration was measured by a modified Lowry method using bovine serum albumin as the standard (Sigma). The protein samples were separated by size in a 7.5% SDS-polyacrylamide gels in duplicate (41). One gel was stained with Coomassie Brilliant Blue R-250, and the other gel was transferred to polyvinylidene difluoride membrane at 500 mA overnight at 4 °C. Western analysis for NuMA (nuclear mitotic apparatus protein) used anti-NuMA monoclonal antibody-1 (mAb-1; recognizes amino acids 900–2100, Oncogene Research Products; 1:500 dilution in PBS), and anti-NuMA mAb-2 (recognizes amino acids 658–691, Oncogene Research Products; 1:100 dilution in PBS) per the manufacturer's instructions. After washing with PBS, the blot was incubated with horseradish peroxidase-conjugated goat anti-mouse IgG (KPL) secondary antibody (1:15,000 dilution in PBS). For detection of SRm160 (SR-related matrix protein of approximately 160 kDa), mAb-B1C8 was used (42); mAb-B1C8 was a gift of Dr. Jeffrey Nickerson (University of Massachusetts, Worchester, MA). After washing with PBS, the blot was incubated with horseradish peroxidase-conjugated goat anti-mouse IgM (KPL) secondary antibody (1:15,000 dilution in PBS plus Tween 20). In other experiments to detect the nonspecific binding, the primary antibody was omitted. Signals were detected using the enhanced chemiluminescence (ECL™) detection kit according to the manufacturer's instructions (Amersham Pharmacia Biotech).

*Probes Designed for the Ribonuclease Protection Assay*—Several probes were designed for use in ribonuclease protection assays (Fig. 1). In all cases, the full-length transcripts were designed to be larger than the protected fragments so that incompletely digested probe could be differentiated from the target signal in the ribonuclease protection assay. All probes were sequenced to verify their structure. The nucleotide distribution in all probes and resulting protected fragments was similar. Two G6PD probes, exon 2-intron 2 and intron 8-exon 9, were made by polymerase chain reaction (PCR) amplification of a genomic clone of G6PD using gene-specific primers and have been described previously (23). The G6PD exon 2-intron 2 probe was shortened by 121 nt by digestion with *Kpn*I. The next probe, which spans exon 8, intron 8, exon 9, and intron 9, was made to detect more than one pre-mRNA. The pBG 2 subclone was made using a G6PD genomic clone (G6PD-B; Ref. 22), which contains a 1.2-kilobase pair *Hin*dIII-*Sac*I fragment spanning intron 7-intron 9. This genomic subclone was digested with *Hin*dIII, *Pst*I, and *Sac*I and the fragment spanning exon 8 to intron 9 was ligated into pBluescript $KS^+$. Prior to use in the probe synthesis reaction, the plasmid was linearized with *Xho*I. The final G6PD probe spans the polyadenylation/cleavage site in the 3′-UTR so it can detect the abundance of polyadenylated RNA after cleavage, as well as uncleaved RNA in a ribonuclease protection assay. DNA was amplified using PCR between the *Xba*I site in the 3′-UTR of the G6PD mRNA and 157 nt downstream of the cleavage site. A *Bpu*1102I site was added to the 3′ primer for cloning purposes. The amplified sequence was ligated into pBluescript $KS^+$, and the plasmid was linearized with *Not*I prior to use in the probe synthesis reaction.

The spot 14 subclone was synthesized from mouse genomic DNA by PCR amplification. The 5′ primer was 5′-GGAATTCGCAGCCTCCATCACATCCTTAC-3′; the underlined sequence is an *Eco*RI site for subcloning followed by spot 14 exon 1 sequence (43). The 3′ primer was 5′-GGGATCCACCGCCATTTATCTCCTCCCTC-3′; the *Bam*HI restriction site for subcloning is underlined and is followed by spot 14 intron sequence (this sequence was kindly provided by Dr. Richard Planells, INSERM, Marseille, France). The β-actin subclone was synthesized from mouse genomic DNA by PCR amplification using the 5′ primer, 5′-GGAATTCGGCAGCGGCTGCTCTTGG-3′ and the 3′ primer, 5′-GGGATCCGCCCACGATGGAGGGGA-3′. The 5′ primer includes an *Eco*RI restriction site (underlined) followed by β-actin intron 1 sequence (this sequence was kindly provided by Dr. Michael Getz, Mayo Clinic, Rochester, MN). The 3′ primer includes the *Bam*HI restriction site (underlined) followed by β-actin exon 2 sequence (44). Following amplification, the DNA fragments were gel-purified and ligated into pBluescript KS$^+$. The β-actin exon protected fragment (114 bp) was too close in size to the spot 14 exon protected fragment (118 bp). Thus, the β-actin clone was cleaved with *Sma*I and *Eco*RI and ligated into pBluescript KS$^+$ restriction sites, resulting in a β-actin exon protected fragment of 90 bp.

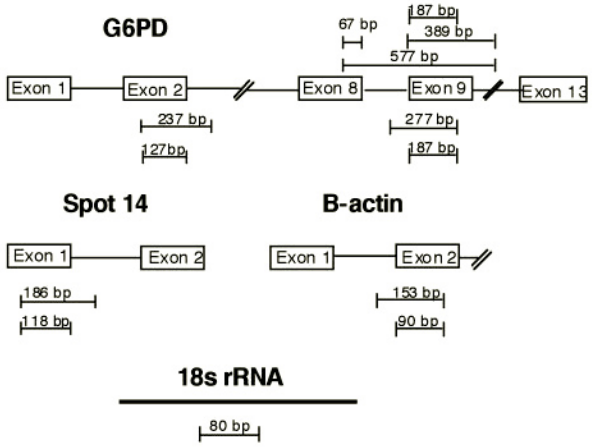


FIG. 1. **Probes and protected fragments for the ribonuclease protection assay.** The *lines* and *boxes* schematically depict the structure of the precursor RNA. In each group of *bars*, the *larger bar* represents the size of the protected fragment in a ribonuclease protection assay when the intron(s) is(are) present and the *smaller bars* are the size of the protected fragments when the intron(s) has(ve) been spliced. A probe for 18 S rRNA was used to demonstrate uniformity of RNA loading. This probe protected an 80-bp fragment.

The 18 S rRNA probe, which was used as a control for RNA loading, was made from pRTI 18 S template (Ambion, Austin, TX). An additional probe was made for chloramphenicol acetyltransferase (CAT) RNA, to check for contamination of cytoplasm RNA into the nuclear fractions. The CAT probe was derived from pRTI CAT (Ambion). To make both sense and antisense CAT RNA, the pRTI CAT template was digested with *Sst*I and *Bam*HI, blunt-ended, and ligated into the *Sma*I site.

*Ribonuclease Protection Assay*—Synthesis of the RNA probes using an *in vitro* transcription reaction and the ribonuclease protection assay were as previously described (23). RNA (20 μg) was hybridized with $2 \times 10^4$ cpm $^{32}$P-labeled each G6PD probe (specific activity ~$10^8$ cpm/μg) and 5000 cpm of 18 S rRNA probe (specific activity ~10,000 cpm/μg) or 7 μg of RNA hybridized with $4 \times 10^4$ cpm each of $^{32}$P-labeled spot 14 and β-actin probe (specific activity ~$10^8$ cpm/μg) at 45 °C for 16 h. The amount of probe was determined empirically to ensure that it was present in molar excess over the transcript. The hybrids protected from digestion with RNase were resolved in a 5% denaturing polyacrylamide gel. The dried gel was placed into a storage phosphor cassette (for 1–3 days). Images were visualized and quantified using ImageQuaNT software (Molecular Dynamics). Statistical analysis in Fig. 5 was done using analysis of variance, and the slopes were tested for parallelism.

*RNase H Blot*—RNase H analysis was done by a modification of the method of Curthoys and Porter (45). Briefly, 30 μg of RNA from the nuclei of starved mice and 15 μg of nuclear RNA from refed mice was mixed with 370 ng of a G6PD specific oligonucleotide (5′-CTAAGGCTCCTCCCCATTGTTCC-3′, nucleotides 1972–1994 of the cDNA sequence) (46). The mixture was heated to 70 °C and then cooled to room temperature over 10 min (47). Digestion with RNase H was for 20 min at 37 °C. The samples were run on a Northern gel, transferred to GeneScreen, and hybridized with a probe to the 3′ end of the G6PD mRNA.

*Cross-contamination Experiment*—Experiments were performed to determine the amount of cytoplasmic RNA present in each nuclear fraction. The 6 ml of homogenization buffer for each liver sample was spiked with 5 ng of *in vitro* synthesized sense CAT RNA. Fractionation was carried out as before. RNA (20 μg) from each fraction was hybridized with $4 \times 10^4$ cpm $^{32}$P-labeled CAT antisense RNA and 5000 cpm 18 S rRNA in a ribonuclease protection assay. The cytoplasmic fraction contained greater than 90% of total cellular RNA, while each nuclear

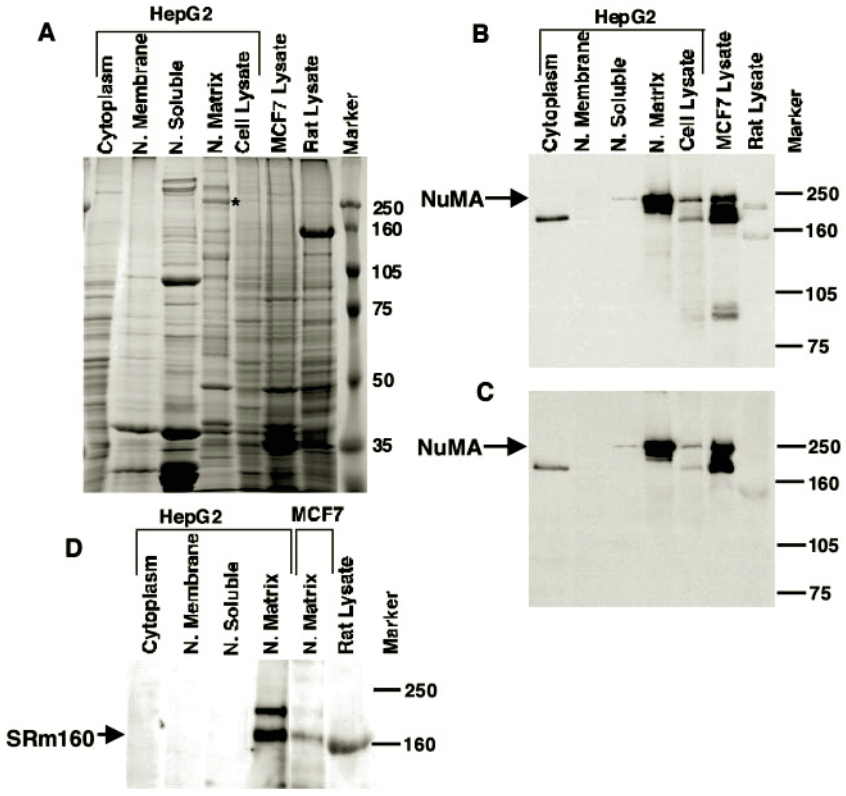


FIG. 2. **SDS-PAGE and Western blot analysis of cellular fractions.** *A*, Coomassie Blue-stained PAGE-separated proteins. Protein (20 μg) from HepG2 cell fractions (except the nuclear soluble fraction, 40 μg) and from the cell lysates were separated by size on 7.5% SDS-PAGE gel and stained with Coomassie Blue. The molecular mass markers are shown in the *last lane*. The *asterisk* indicates a band, which migrates at the size of NuMA. Western blot analysis of cellular fractions using anti-NuMA mAb-1 (*B*) and anti-NuMA mAb-2 (*C*). Protein (20 μg) from HepG2 cell fractions (except nuclear soluble fraction, 40 μg), along with 20 μg of protein from HepG2, MCF7, and rat hepatocyte cell lysate were separated by size on a 7.5% polyacrylamide gel before transfer to polyvinylidene difluoride membrane, antibody staining, and detection as described under "Materials and Methods." The *arrow* indicates the position of NuMA. The *numbers* on the *right* are the sizes of the molecular mass markers in kDa. *D*, Western blot analysis of cellular fractions using mAb-B1C8. Protein (20 μg) from HepG2 cell fractions, HepG2 cell lysate, MCF7 nuclear matrix, and rat hepatocyte lysate were separated by size, transferred and stained as described under "Materials and Methods." The size of the antigen SRm160 is shown on the *left side* of the blot.

fraction contained ~2% of the total cellular RNA. After correction for these differences in RNA abundance between cellular fractions, 97% of CAT RNA was retained in the cytoplasm, less than 1% of the CAT RNA was in the nuclear membrane and nuclear soluble fractions, and less than 0.01% was in the nuclear matrix fraction. These data indicate that the cytoplasmic RNA contribution to the signal for spliced RNA in the nuclear fractions was quite low.

## RESULTS

*Isolation of the Insoluble Nuclear Fraction*—Regulation of G6PD expression occurs at a step after transcription but prior to the exit of the mRNA from the nucleus (23). Thus, the potential regulatory step is during RNA processing. To measure G6PD RNA accumulation during processing, we used sequential extraction of cells with detergent, DNase I, and salt to isolate the insoluble nuclear fraction. Isolation of this fraction provides an experimental tool to measure pre-mRNAs that are both newly synthesized and undergoing processing (28, 33, 48). Further, RNA in the processing pathway is separated from mature RNA at the nuclear pore. Historically, this fraction was called the nuclear matrix, and we will use this term for simplicity. To validate our protocol, we used Western analysis with antibodies against two proteins, NuMA and SRm160, which are associated with the nuclear matrix (42, 49). Staining should only occur against proteins of the expected size within the nuclear matrix fraction. Appearance of these proteins in the nuclear soluble and/or the nuclear membrane factions would indicate that the detergent was extracting the nuclear matrix.

NuMA, also known as centrophilin (50), SPN (49), and SP-H (51), is an ~240-kDa nuclear protein that resides at the spindle poles during mitosis and is required for processing of precursor mRNA during interphase (52, 53). Monoclonal antibodies raised against NuMA (mAb-1 and mAb-2) only react with human NuMA antigen, thus, HepG2 cells were used as a source of the cellular fractions. A different pattern of protein distribution was observed in each cellular fraction upon staining the gel with Coomassie Blue (Fig. 2*A*). An abundant nuclear protein (*asterisk* in Fig. 2*A*) represents NuMA as confirmed by Western analysis. Staining of the proteins in the cellular fractions with NuMA mAb-1 detected its antigen (~240 kDa) predominantly in the nuclear matrix fraction (Fig. 2*B*). The identity of this protein as NuMA was confirmed with a second antibody to a different epitope on the protein (Fig. 2*C*). Two additional bands (approximately194 and 195 kDa) were detected in this fraction corresponding to two additional isoforms of NuMA (54, 55). A minor amount of NuMA was detected within the nuclear soluble fraction, but only when twice as much protein was loaded onto the gel from this fraction as compared with the other cellular fractions (Fig. 2*B*). The amounts of protein loaded on the gel represent nearly all of the nuclear soluble fraction and half of the nuclear matrix fraction. As expected, NuMA was detected in HepG2 and MCF7 cell lysates, but not in rat hepatocytes, which was included as a negative control. Smaller bands at ~160 and 180 kDa represent nonspecific binding (data not shown; Refs. 52, 53, and 56).

A second nuclear matrix protein was detected using the monoclonal antibody, B1C8, which recognizes SRm160, an SR protein required for mRNA splicing (57, 58). Western blot analysis using B1C8, detected a 160–180 kDa specific protein (42), only in the HepG2 and MCF7 nuclear matrix fractions, but was not detected in the cytoplasm, nuclear membrane, and nuclear soluble fractions (Fig. 2*D*). The band detected at ~160 kDa in the rat hepatocyte lysate appeared to be nonspecific and was also observed during staining with anti-NuMA antibodies (Fig. 2, *A* and *B*). Thus, the retention of SRm160 and NuMA within the nuclear matrix fraction indicated that this subcellular structure was not extracted to any great extent into other fractions during the isolation protocol.

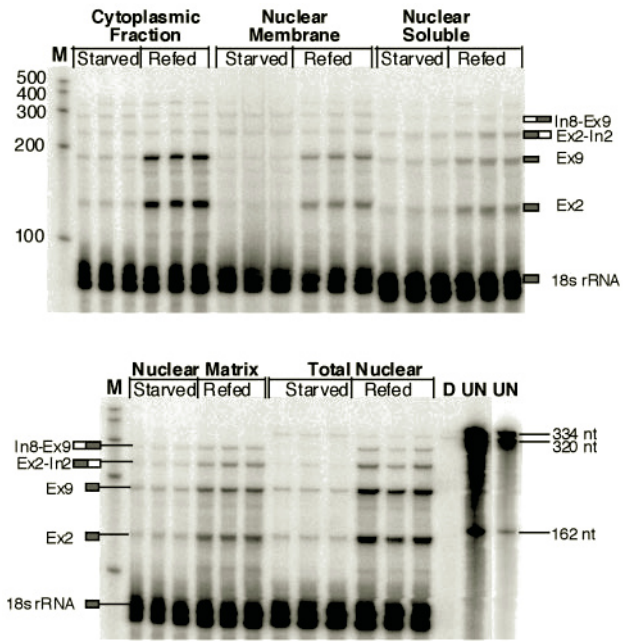


FIG. 3. **Effects of starvation and refeeding on G6PD mRNA abundance in each cellular fraction.** Mice were provided access to the high carbohydrate, low fat diet *ad libitum* for 1 week. After 24 h of starvation, 6 mice were sacrificed (starved) and the high carbohydrate, low fat diet was returned to the other 6 mice for 24 h (refed). The livers from 3 mice from each group were fractionated and the other 3 livers were used to isolate nuclear RNA. RNA (20 $\mu$g) from cellular fractions (or 20 $\mu$g of nuclear RNA) was hybridized with each of the G6PD probes (exon 2-intron 2 and intron 8-exon 9) and the 18 S rRNA probe in a ribonuclease protection assay as described under "Materials and Methods." Each *lane* represents a cellular fraction from a single mouse. The size of G6PD exon 2-intron 2, G6PD intron 8-exon 9, and 18 S rRNA full-length probes are 334, 320, and 162 nt, respectively. The positions of the protected fractions for G6PD exon 2-intron 2 (*Ex2-In2*), exon 2 (*Ex2*), and G6PD intron 8-exon 9 (*In8-Ex9*), exon 9 (*Ex9*), and 18 S rRNA are shown. *D*, digested control (hybridization of 30 $\mu$g of yeast RNA with both probes followed by RNase digestion). *UN*, undigested control (hybridization of 30 $\mu$g of yeast RNA with both probes without RNase digestion). Only 5% of the undigested control reaction was loaded onto the gel. *M*, RNA marker in nucleotides. These data are representative of three independent experiments that showed similar results.

*Effects of Starvation and Refeeding on G6PD mRNA Abundance in Each Cellular Fraction*—Starvation and refeeding produce the greatest changes in the amount of G6PD mRNA in both the cytoplasm and the nucleus (23). Thus, we used this dietary paradigm to determine changes in the amounts of G6PD pre-mRNA during processing. We used two probes, separated by 12 kilobase pairs, to detect G6PD RNA. Each probe hybridized across an exon-intron junction and resulted in two protected fragments (Figs. 1 and 3). The longer fragment (exon 2-intron 2; intron 8-exon 9) corresponds to unspliced RNA that contains both the exon and intron sequences; the smaller fragment (exon 2; exon 9) corresponds to spliced RNA that only contains the exon sequences. The terms unspliced and spliced must be used cautiously because each probe provides information about the splicing of only 1 of the 12 introns in the G6PD gene.

In these and later experiments, a probe for 18 S rRNA was included in the reactions to control for RNA loading in the RNase protection assay. 18 S rRNA was present in all the cellular fractions (Fig. 3). The variation in 18 S rRNA amounts between lanes was less than 15% in this (Fig. 3) and later figures. Significant amounts of 18 S rRNA were observed within the insoluble fraction of the nucleus. The large amounts in the nuclear membrane and nuclear soluble fractions most likely represent movement of 18 S rRNA through the nucleus

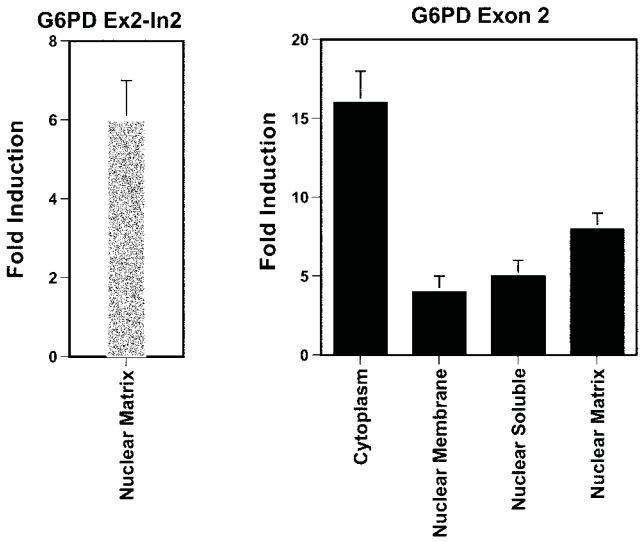


FIG. 4. **The -fold induction of G6PD mRNA abundance in each cellular fraction due to refeeding.** This figure shows the cumulative results of three independent experiments carried out as described in the legend to Fig. 3. The amounts of the two G6PD protected fragments (exon 2 and exon 2-intron 2 (*Ex2-In2*)) were quantified in each of the cellular fractions from the livers of starved and refed mice (mean ± S.E., representing 10 mice). Each *bar* represents the value (in ImageQuaNT units) of each protected fragment in that fraction from refed mice divided by the value of that protected fragment in the same cellular fraction from starved mice.

as well as cytoplasmic contamination of these fractions.

In refed mouse liver, unspliced G6PD mRNAs were detected in greatest abundance in the nuclear matrix fraction and to a lesser extent in the nuclear soluble and nuclear membrane fractions (Fig. 3). We detected a very small portion of G6PD pre-mRNA in the cytoplasm. This is the result of rupture of the nucleus during the fractionation due to the low temperature (−20 °C) used; pre-mRNA in the cytoplasm was not observed when the fractionation was performed at 4 °C (data not shown). Curiously, nuclear matrix proteins were not detected in the cytoplasm (Figs. 2, *B–D*). This may reflect that pre-mRNAs are less tightly associated with the nuclear matrix fraction than the protein components. Regardless, the majority of the pre-mRNA was localized to the nucleus.

Consistent with our previous results (22, 23), the abundance of G6PD mRNA in the cytoplasm was very low after 24 h of starvation as measured with the exon 2 and exon 9 protected fragments (Fig. 3). Refeeding the starved mice caused a 16–20-fold increase in the abundance of G6PD mRNA in the cytoplasm (Fig. 4). During starvation, the amount of G6PD mRNA was uniformly low in all nuclear fractions regardless of the extent of processing of the mRNA. Upon refeeding, the amount of G6PD unspliced RNA (exon 2-intron 2 and intron 8-exon 9) increased 6-fold in the nuclear matrix fraction (Fig. 4). The amount of unspliced RNA on the nuclear matrix could account for nearly all of this class of RNA in total nuclear RNA (Fig. 3). An increase of 2-fold or less in G6PD unspliced RNA was also observed in the nuclear soluble and nuclear membrane fractions, but the amount of unspliced RNA was close to detection limits. Refeeding resulted in an 8-fold increase in the abundance of G6PD spliced RNA (exon 2 and exon 9) on the nuclear matrix (Figs. 3 and 4). Although the -fold increase in spliced *versus* unspliced G6PD mRNA abundance did not vary significantly, the absolute amounts of spliced *versus* unspliced RNA were substantially different. In the refed mice, the amount of spliced RNA was 11-fold greater than the amount of unspliced RNA (2334 ± 290 *versus* 212 ± 40 phosphorimager units/nt for spliced *versus* unspliced RNA; exon 2-intron 2 probe). An increased amount of spliced RNA was also observed in the nuclear soluble and nuclear membrane fractions. Similar results were observed with G6PD intron 8-exon 9 probe in all experiments (Fig. 3). Thus, starvation and refeeding resulted in changes in the amount of G6PD pre-mRNAs in the processing pathway, and the amount of spliced G6PD RNA was consistently greater than the amount of unspliced RNA.

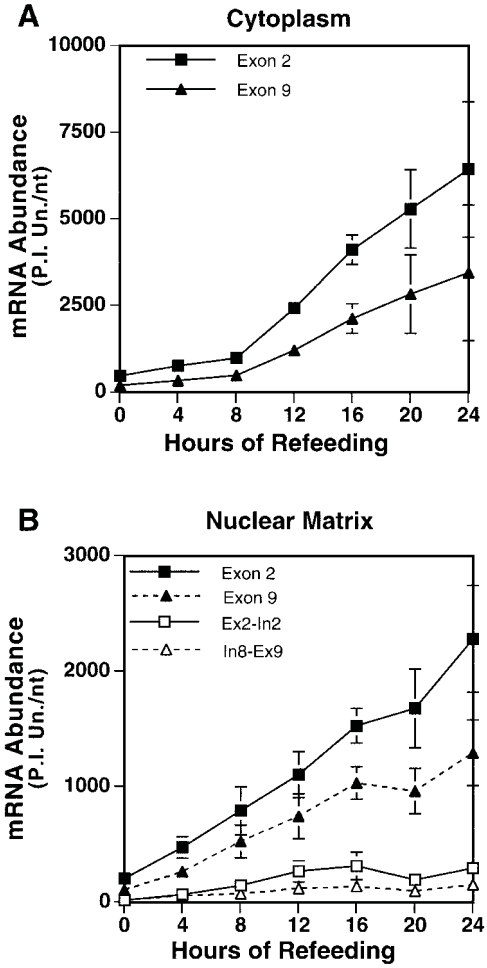


FIG. 5. **Kinetics of G6PD mRNA accumulation in the cytoplasm (*A*) and the nuclear matrix (*B*) during 24 h refeeding.** Mice ($n$ = 28) were provided access to the low fat diet *ad libitum* for 1 week. After 24 h of starvation, the low fat diet was returned for up to 24 h (refeeding period). Four mice were sacrificed every 4 h up to 24 h, starting at time point 0 (starved mice). The livers were removed from the mice, fractionated and RNA was isolated from each fraction (see "Materials and Methods"). *A*, RNA from the cytoplasmic fraction (20 μg) from each mouse liver was hybridized with the two G6PD probes (exon 2-intron 2 and intron 8-exon 9) and the 18 S rRNA probe in a ribonuclease protection assay. The amounts of G6PD spliced RNA, exon 2 (*Ex2*), and exon 9 (*Ex9*) protected fragments were quantified using ImageQuaNT software and the resulting values were adjusted for the size of the protected fragment. Each point represents the mean ± confidence interval ($n$ = 4 mice/time point except the 24-h time point with $n$ = 6 mice; 90% confidence). *P.I. Un.*, phosphorimage units. *B*, RNA (20 μg) from the nuclear matrix fractions of each mouse liver was hybridized with the G6PD and 18 S rRNA probes (as above) in a ribonuclease protection assay. Amounts of G6PD spliced RNA (*Ex2*, and *Ex9* protected fragments) and unspliced RNA, exon 2-intron 2 (*Ex2-In2*) and intron 8-exon 9 (*In8-Ex9*) protected fragments were quantified using ImageQuaNT software; each value was divided by the size of the fragment. Each point represents the mean ± confidence interval ($n$ = 4 mice/time point except the 24-h time point with $n$ = 6 mice; 90% confidence). In some cases the confidence interval bars do not extend beyond the size of the symbol.

*Kinetics of G6PD mRNA Accumulation in Cytoplasm and Nuclear Matrix during 24-h Refeeding*—Changes in the amount of G6PD spliced RNA in the nucleus could be caused by

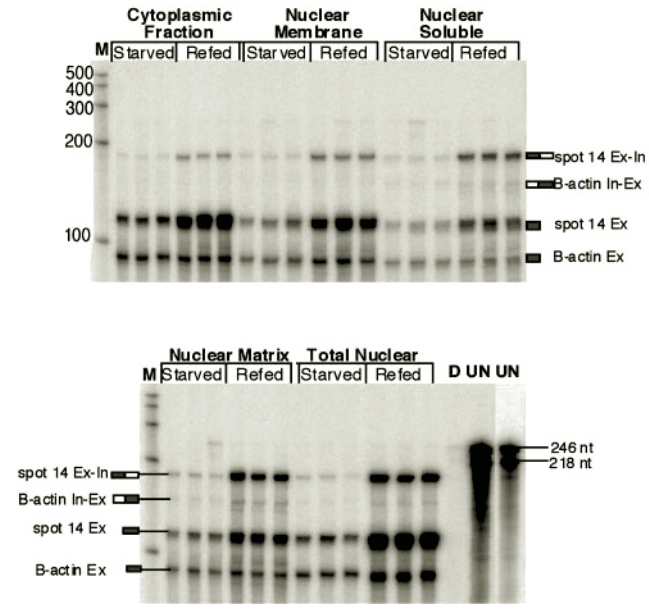


FIG. 6. **Effects of starvation and refeeding on the spot 14 and β-actin mRNA abundance in the cellular fractions.** RNA (7 μg) isolated from cellular fractions or nuclear RNA (from same mouse livers as in Fig. 4) was hybridized with the spot 14 and β-actin probes in a ribonuclease protection assay. Each lane represents a cellular fraction from a single mouse. The size of spot 14 exon 1-intron 1 and β-actin intron 1-exon 2 full-length probes are 246 and 218 nt, respectively. The positions of the protected fragments for spot 14 exon 1-intron 1 (*Ex-In*) and exon 1 (*Ex*), and for β-actin intron 1-exon 2 (*In-Ex*) and exon 2 (*Ex*) are shown. *D*, digested control (hybridization of 7 μg of yeast RNA with both probes followed by RNase digestion). *UN*, undigested control (hybridization of 7 μg of yeast RNA with both probes without RNase digestion). Only 5% of the undigested control reaction was loaded onto the gel; a lighter exposure of undigested was included for clarity. *M*, RNA markers in nucleotides. These data are representative of three independent experiments that showed similar results.

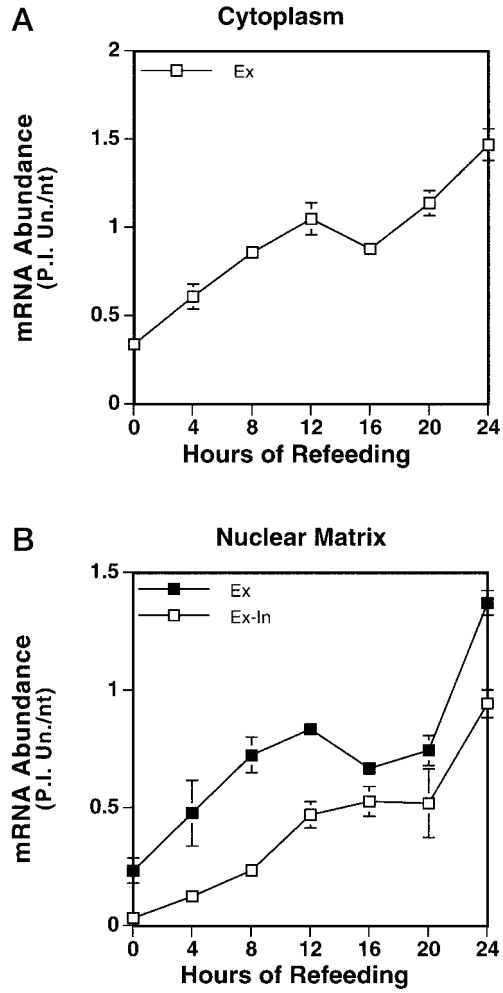


FIG. 7. **Kinetics of spot 14 mRNA accumulation in the cytoplasm (*A*) and the nuclear matrix (*B*) during 24 h refeeding.** *A*, RNA (7 μg) from the cytoplasmic fraction from each mouse liver (same mice as in Fig. 6) was hybridized with the spot 14 probe in a ribonuclease protection assay. The amount of spot 14 spliced mRNA (*Exon*) protected fragment was quantified using ImageQuaNT software. Each point represents the mean ± S.E. ($n = 4$ mice/time point except the 24-h time point with $n = 6$ mice). *B*, RNA (7 μg) from the nuclear matrix fraction from each mouse liver (as above) was hybridized with the spot 14 probe in a ribonuclease protection assay. The amounts of spot 14 spliced mRNA (*Ex*) and precursor mRNA (*Ex-In*) protected fragments, were quantified using ImageQuaNT software and corrected for the size of the protected fragment. The values are normalized to β-actin to correct for loading differences; β-actin expression did not vary during this time course (data not shown). Each point represents the mean ± S.E. ($n = 4$ mice/time point except the 24-h time point with $n = 6$ mice). In some cases the S.E. bars do not extend beyond the size of the symbol. *P.I. Un.*, phosphorimage units.

changes in either the rate of its production due to processing of the nascent transcript or degradation of this pool of mRNA. To further investigate the differences in the amount of G6PD unspliced *versus* spliced RNA, we measured mRNA accumulation with time during refeeding. In mice that had been starved for 24 h (0 time point), the amount of G6PD mRNA was very low in both the cytoplasm and the nuclear matrix fractions (Fig. 5, *A* and *B*). In the cytoplasm, accumulation of G6PD mRNA occurred with two different rates. During the first 8 h, G6PD mRNA increased 3-fold but at a slow rate (Fig. 5*A*). An increase of 12–16-fold was observed 24 h after refeeding, and the rate of accumulation was faster between 8 and 24 h. In the nuclear matrix fraction, G6PD unspliced RNA was present in very low abundance at all time points, consistent with the lack of transcriptional regulation of this gene. The amount of unspliced RNA accumulated at a linear rate ($r = 0.99$) of ~22 and 7 units/h (exon 2-intron 2 and intron 8-exon 9, respectively) over 16 h of refeeding (Fig. 5*B*). This small increase is due to splicing at other intron/exon boundaries not measured by these probes. A 3–4-fold increase was observed in the rate of accumulation of G6PD spliced RNA compared with unspliced RNA accumulation during the same period (86 and 63 units/h, for exon 2 and exon 9, respectively). This rate was linear ($r = 0.99$) over 16 h of refeeding but continued to increase through 24 h. Furthermore, these increases in rate between the spliced and unspliced pools of RNA were significant ($p < 0.0001$ for both exon 2-intron 2 *versus* exon 2 and intron 8-exon 9 *versus* exon 9). At all time points, the amount of G6PD unspliced RNA was markedly less than the amount of spliced RNA (Fig. 5*B*); however, both pools of RNA increased during refeeding. The more rapid accumulation of spliced RNA suggests that refeeding enhances the rate of production of this RNA.

*Effects of Starvation and Refeeding on Spot 14 and β-Actin mRNA Abundance in Each Cellular Fraction*—The nuclear posttranscriptional regulation observed with the G6PD gene is not a commonly described mechanism. To determine whether related and unrelated genes share this mechanism, we measured the changes in the abundance of precursor and mature mRNA for a gene that is transcriptionally regulated in response to starvation and refeeding and a gene that is unregulated by this dietary paradigm. The spot 14 gene undergoes large changes in its transcription rate in response to dietary and hormonal stimuli (59, 60). In addition, spot 14 mRNA abundance is also regulated posttranscriptionally (61–63). Spot 14 contains only one intron, thus, the protected fragments corresponding to unspliced (exon 1-intron 1) and spliced (exon

1) represent the spot 14 precursor and mature mRNA, respectively (Fig. 1; Ref. 64). The amounts of both unspliced and spliced spot 14 mRNA were very low in the livers starved mice. Refeeding increased both the unspliced and spliced RNA in the nucleus and the mature mRNA in the cytoplasm (Fig. 6). In contrast to G6PD, the ratio of unspliced to spliced spot 14 mRNA was much greater. In this regard, the amount of unspliced RNA on the nuclear matrix was 63% or more of the amount of spliced spot 14 mRNA in this fraction.

β-Actin, a constitutively expressed gene, is not involved in intermediary metabolism and is not regulated to any great extent by these nutritional manipulations (22). We detected a very small amount of β-actin unspliced RNA in the livers of starved and refed mice, whereas the amount of spliced RNA was clearly detectable in all cellular fractions (Fig. 6). The amount of β-actin spliced RNA in each cellular fraction was increased 2-fold after refeeding; however, marginal changes in the amount of β-actin mature mRNA due to dietary manipulation were not unexpected (65). The physiological relevance of this increase in actin expression is not clear. The increase in expression was detectable by 4 h of refeeding and the amount of actin mRNA (both unspliced and spliced) remained constant over the 24 h of refeeding (data not shown). Changes in the transcriptional activity of the actin gene are not seen throughout this time period (22). Despite the absence of large changes in the expression of the β-actin gene due to nutritional status, the ratio of unspliced to spliced RNA for this gene resembled that of G6PD and not the transcriptionally regulated spot 14 gene.

*Kinetics of Spot 14 mRNA Accumulation in Cytoplasm and Nuclear Matrix during 24-h Refeeding*—The amounts of unspliced *versus* spliced RNA on the nuclear matrix were clearly different between spot 14, which is transcriptionally regulated by dietary status, and G6PD, which is not regulated transcriptionally. We next examined the kinetics of spot 14 mRNA accumulation in the cytoplasm and the nuclear matrix. Enhanced accumulation of spot 14 mature mRNA was detected in the cytoplasm as early as 4 h after refeeding and increased accumulation continued through 24 h (Fig. 7*A*). In the nuclear matrix fraction, the abundance of spot 14 unspliced RNA increased dramatically with refeeding (Fig. 7*B*). This increase is consistent with an increase in production of this mRNA due to transcriptional regulation of the gene (60) and is in sharp contrast to the changes in unspliced RNA abundance with G6PD, which does not undergo transcriptional regulation. However, at all time points, the amount of spliced RNA exceeded the amount of unspliced RNA. This increase in spliced mRNA compared with unspliced is consistent with previous reports (61). Thus, transcriptional regulation of spot 14 appears to be coupled with posttranscriptional changes in the rate of mature mRNA formation. Enhanced processing of mRNA may be a common mechanism for nutritional regulation of gene expression.

*Effects of Starvation and Refeeding on Accumulation of G6PD Splicing Intermediates*—We next sought to distinguish if stabilization of the message is occurring during processing itself or if it is the fully spliced form of the message that is stabilized. A probe was designed that contained two introns and thus detected pre-mRNA at three different stages in splicing: 1) both introns present, 2) removal of only one of the two introns, and 3) removal of both introns. As illustrated in Fig. 8, hybridization of G6PD pBG 2 probe, which spans two consecutive exon-intron boundaries (exon 8-intron 8-exon 9-intron 9), with nuclear matrix mRNA resulted in detection of four protected fragments (Fig. 8). The exon 8-intron 8-exon 9-intron 9 (*A*) protected fragment represents mRNA in which both introns

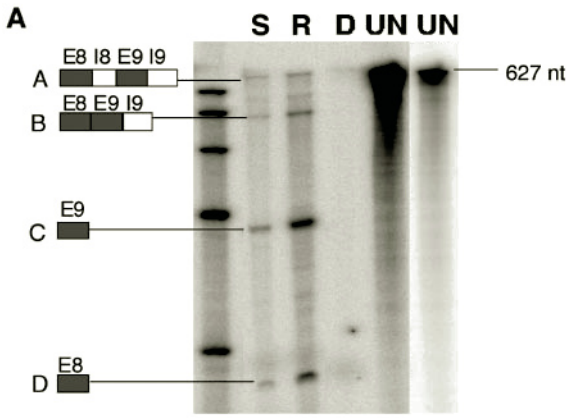


B

| Protected Fragment | Starved | Refed |
|---|---|---|
| | P.I. Un./nt | |
| A | 79 | 98 |
| B | 83 | 273 |
| C | 380 | 1977 |
| D | 537 | 2830 |
| | Ratio | |
| B/A | 1 | 3 |
| C/A | 5 | 20 |
| D/A | 7 | 29 |

FIG. 8. **Effects of starvation and refeeding on accumulation of G6PD splicing intermediates.** RNA was isolated from starved or refed mice as explained in the legend to Fig. 3. *A*, RNA (20 μg) from nuclear matrix fractions was hybridized with G6PD pBG 2 probe, which spans the exon 8, intron 8, exon 9, and intron 9 in ribonuclease protection assay. The size of pBG 2 full-length probe (627 nt) is shown on the *right*. The protected fragments include G6PD exon 8-intron 8-exon 9-intron 9 (*E8 I8 E9 I9*, 577 nt) (*A*), G6PD exon 8-exon 9-intron 9 (*E8 E9 I9*, 389 nt) (*B*), G6PD exon 9 (*E9*, 187 nt) (*C*), and G6PD exon 8 (*E8*, 67 nt) (*D*). At the top of the gel, *D* represents digested control (hybridization of 30 μg of yeast RNA with both probes followed by RNase digestion) and *UN* represents undigested control (hybridization of 30 μg of yeast RNA with probe without RNase digestion). Only 5% of the undigested control reaction was loaded onto the gel. *M*, RNA marker as in Fig. 6. *Panel A* is representative of a single starved and refed mouse; data from three other starved and refed mouse showed similar results. *Panel B*, each protected fragment from *A* was quantified using ImageQuaNT software as phosphorimage units (*P.I. Un.*). The phosphorimage units were divided by the length of each protected fragment (nt). The ratio of each splicing intermediate species (*B*, *C*, and *D*) to unspliced pre-mRNA (*A*) is shown. These results are similar to three additional experiments using total nuclear RNA (M. A. Gibson and L. M. Salati, unpublished data).

are still present. The G6PD exon 8-exon 9-intron 9 (*B*), exon 9 (*C*), and exon 8 (*D*) protected fragment represents successive removal of intron 8 and then intron 9 (Fig. 8). A protected fragment representing removal of intron 9 but containing intron 8 (375 nt) was not detected, indicating that order of intron removal was intron 8 followed by intron 9. Successive removal of introns from the mRNA resulted in an increase in the amount of spliced RNA for G6PD both in refed and starved state. However, even RNA from which only one of the two detectable introns had been spliced was increased in amount relative to RNA that contained both introns. A greater increase was observed in the amount of RNA from which two introns had been spliced. A similar observation was made in four additional experiments using nuclear RNA (data not shown). Comparison of the amounts of partially spliced mRNA during starvation and refeeding indicated that refeeding stimulated a greater accumulation of this intermediately spliced mRNA (*B*/*A* 2.8 *versus* 1.1). Continued splicing further stimulated RNA accumulation (*C*/*A* 20.2 *versus* 4.8; *D*/*A* 28.9 *versus* 6.8). Thus, the regulated increase in G6PD RNA accumulation in-

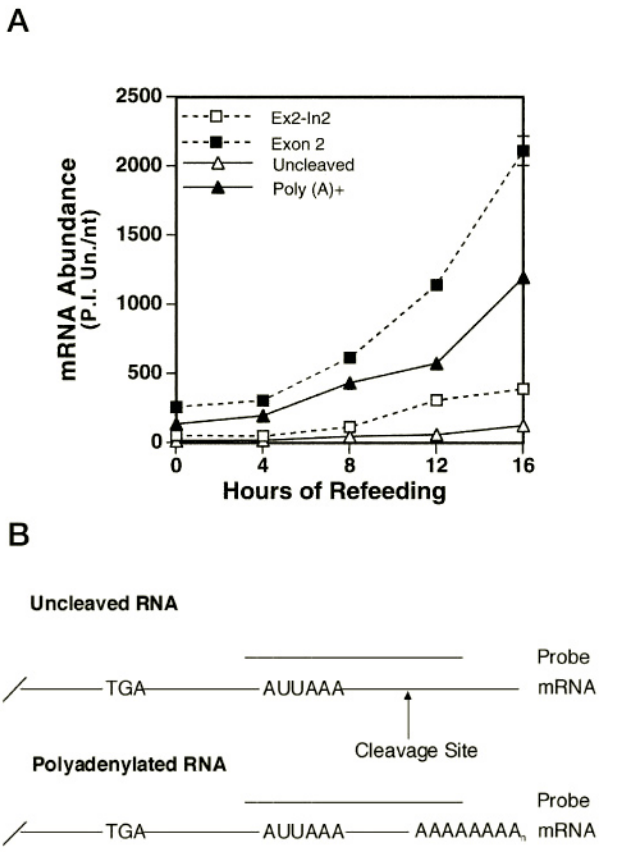


FIG. 9. **The effects of refeeding on the G6PD mRNA 3′ end processing.** The animal handling and the RNA isolation were the same as described in the legend to Fig. 5. *A*, nuclear matrix RNA isolated from 3–4 mice at each time point (0, 4, 8, 12, and 16 h of refeeding) was pooled and used in ribonuclease protection assays. RNA was hybridized with G6PD exon 2-intron 2 (*Ex2-In2*) and 3′-UTR probes. *B*, the 3′-UTR probe hybridizes to a region 138 nt upstream and 150 nt downstream of the polyadenylation/cleavage site. RNA hybridization with the 3′-UTR probe resulted in two protected fragments, pre-mRNA that are not yet cleaved (unpolyadenylated RNA), and the cleaved RNA (therefore polyadenylated RNA). The abundance of each protected fragment was quantified using ImageQuaNT software and corrected for the length of the protected fragment.

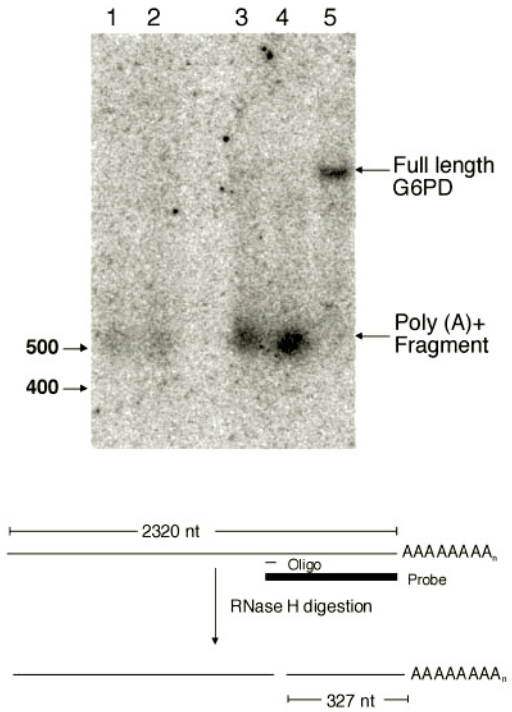


FIG. 10. **Nutritional status does not regulate the length of the G6PD poly(A) tail.** Nuclear RNA was isolated from mice that had been starved for 24 (*lanes 1* and *2*) or from mice that had been starved and then refed the high carbohydrate diet for 24 h (*lanes 3*, *4*, and *5*). RNA was hybridized with a G6PD-specific oligonucleotide (*lanes 1–4*) or without the oligonucleotide (*lane 5*). Following RNase H digestion, the products were separated by size on a Northern gel and probed with a G6PD probe for sequences 3′ of the digestion site. The *markers* on the *right* side of the figure indicate the positions of the full-length G6PD mRNA and the 3′-fragments containing G6PD sequence and the poly(A) tail. The *numbers* on the *left* of the figure indicate the size of the molecular weight markers. This experiment was repeated four times with the same results.

volves events earlier in the RNA processing pathway and not merely stabilization of the mature mRNA.

*Effects of Refeeding on the 3′ End Processing of the G6PD mRNA*—Events early in processing that could regulate pre-mRNA accumulation include splicing and 3′ end formation (cleavage and polyadenylation). To distinguish between these two possibilities, we measure the accumulation of uncleaved *versus* polyadenylated RNA during refeeding. A probe to the 3′-UTR was hybridized with RNA samples from starved and refed mice. The 3′-UTR probe resulted in the detection of two protected fragments. A protected fragment of 288 nt corresponded to uncleaved pre-mRNA (therefore unpolyadenylated RNA). The second protected fragment (138 nt), represented the polyadenylated mRNA (Fig. 9). Cleaved mRNA that had not been polyadenylated was not detected.[2] The abundance of uncleaved pre-mRNA was very low both in starved mice and in mice after 16 h of refeeding, suggesting that this species of mRNA was being synthesized at a basal level and accumulating very slowly during refeeding (rate of 8 phosphorimage units/h, $r = 0.95$). The G6PD intron 2-exon 2 probe was used with the same aliquot of mRNA as a control to compare with previous results. The abundance of polyadenylated mRNA increased 8-fold similar to the G6PD unspliced mRNA (exon 2-intron 2 protected fragment) with refeeding. Likewise, the rate of accumulation of the polyadenylated RNA was similar to that for unspliced RNA during the first 12 h of refeeding (slope of 78 ($r = 0.95$) *versus* 30 ($r = 0.98$) for polyadenylated and exon 2-intron 2, respectively). In contrast, the rate of accumulation of spliced mRNA (exon 2 protected fragment) was 149 ($r = 0.97$), nearly twice the rate of polyadenylated RNA accumulation. Consistent with previous results, the amount of unspliced mRNA (exon 2-intron 2 protected fragment) was 25% of the amount of spliced mRNA. Thus, accumulation of G6PD mRNA requires polyadenylation but the rate of accumulation of this pool of RNA is not sufficient to account for the enhanced rate of mature RNA formation during refeeding.

To further verify that events involved in the formation of the 3′ end of G6PD mRNA, the length of the poly(A) tail was measured. Shortening of the poly(A) tail can destabilize mRNA (*cf.* Refs. 66 and 67). Nuclear RNA isolated from the livers of mice that had been starved or starved and then refed was subjected to RNase H analysis (Fig. 10). The size of the 3′ fragment resulting from RNase H digestion was slightly greater than 500 nt. Of this sequence, 327 nt corresponds to the G6PD 3′-UTR and the remaining 173 or more nucleotides represent the poly(A) tail. Starvation and refeeding did not alter the length of the poly(A) tail. Taken together, these results indicate that the rate of formation of the 3′ end of the G6PD mRNA is not affected by dietary status. Thus, regulation of G6PD by starvation and refeeding is due to changes in the efficiency at which the pre-mRNA is spliced.

[2] C. D. Shrader and L. M. Salati, unpublished data.

## DISCUSSION

Hepatic G6PD activity and mRNA abundance undergo large changes with dietary manipulations both *in vivo* and in primary hepatocyte cultures (22, 38). In this study, we present our results that the efficiency of RNA splicing is the step regulating G6PD pre-mRNA accumulation during refeeding. Several lines of evidence indicate that splicing is the step regulating G6PD RNA accumulation. The following model summarizes this regulation.

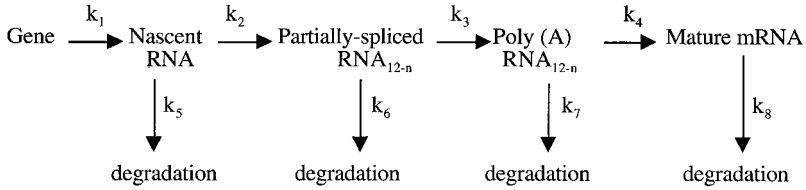


SCHEME I

The reactions are listed in this order for illustration purposes only. Splicing and polyadenylation occur cotranscriptionally (35, 68); thus, splicing ($k_2$ and $k_4$) and polyadenylation ($k_3$) are most likely occurring coincidentally.

In previous reports from our laboratory, we demonstrated that the transcriptional activity ($k_1$) of the G6PD gene is not regulated by starvation or refeeding and in fact of the rate of G6PD transcription is very low. However, refeeding results in increases in the accumulation of both partially spliced and mature forms of G6PD mRNA in the nucleus. Thus, regulation of G6PD expression is occurring at a posttranscriptional step in the nucleus. Nuclear posttranscriptional regulation can involve changes in the rate of degradation of the RNA (*i.e.* $k_{5-8}$) or regulation of the efficiency of steps in processing (*i.e.* $k_{2-4}$) of the primary transcript. The rate of degradation of a mRNA can be regulated by both the presence of a poly(A) tail and the length of this tail. In this regard, the rate of accumulation of nonpolyadenylated RNA ($k_2$) was the slowest of all measured, but did increase during refeeding (Fig. 9). The increase in the rate of accumulation of polyadenylated RNA ($k_3$) was insufficient to account for the overall rate of accumulation of mature mRNA in the nucleus. We also examined the structure of the 3′ end of G6PD RNA and found no difference in the length of the poly(A) tail between the starved and refed states (Fig. 10). Thus, the rate of degradation ($k_7$) would be unchanged by these nutritional manipulations. These results indicate that polyadenylation of the RNA while necessary for accumulation of G6PD RNA does not cause the high rates of accumulation of G6PD mRNA during refeeding. It is during the splicing of G6PD pre-mRNA that the greatest increases in rate were observed ($k_2$ and $k_4$), and it is the rate of accumulation of the fully processed RNA ($k_4$) that was most enhanced (Figs. 5, 8, and 9). During starvation, splicing is not enhanced and the decrease in the rates of $k_2$ and $k_4$ will result in enhanced degradation of the G6PD transcripts in the nucleus ($k_6$ and $k_7$). Once fully processed, G6PD mRNA is stable in the nucleus and no change in its rate of degradation ($k_8$) is detectable across dietary manipulations (23).

The precise structure with respect to numbers of introns remaining in the RNA that is stabilized is not known. The G6PD gene is 18 kilobase pairs and contains 12 introns. Since splicing is most likely occurring cotranscriptionally, most certainly the stabilized RNA is partially spliced. Curiously, the amount of RNA detected with the more 5′ probe (exon 2-intron 2) was consistently greater than the amount measured with the more 3′ probe (intron 8/exon 9) and the rate of accumulation of the RNA was slightly greater when measured with the 5′-most probe (Fig. 5). The simplest explanation is that this reflects differences in specific activity of the probes and/or their hybridization efficiency. Alternatively, it may reflect an important regulatory phenomenon. Discriminating between these alternatives will require precise mapping of the regulatory element(s) and is the subject of current investigations in the laboratory.

The failure to accumulate G6PD pre-mRNA in the starved mouse suggests that transcripts that fail to be fully processed are degraded within the nucleus. In this regard, mutations thateffect splicing or polyadenylation result in degradation of the RNA in the nucleus (37, 69). Degradation of the partially spliced G6PD transcript must be rapid and most likely takes place while the nascent transcript is at the site of transcription because we did not detect any increase in the abundance of pre-mRNA in other nuclear fractions from the livers of starved mice (Fig. 3). Even in the starved state, G6PD expression is still required for cell viability (70). Thus, even at low levels of G6PD expression, the increase in spliced RNA relative to unspliced RNA was detectable.

Only a few examples have been reported of nuclear posttranscriptional regulation. These include expression of fibronectin (71), alkaline phosphatase (72, 73), interleukin-2 (74), tumor necrosis factor-$\alpha$ (75), peptidylglycine $\alpha$-amidating monooxygenase (76), and spot 14 (61). Regulation of fibronectin expression by dexamethasone involves changes in pre-mRNA amounts without changes in transcription rate of the gene (71). In the case of the alkaline phosphatase gene, its pre-mRNA is only processed to mature mRNA when the cells are treated with retinoic acid (73). During T cell activation, mitogens stimulate expression of the interleukin-2 gene by stimulated the accumulation of precursor transcripts for interleukin-2 in the nucleus, in the absence of transcriptional changes (74). Similarly, tumor necrosis factor-$\alpha$ mRNA is also induced during T cell activation by changes in the efficiency of its splicing (75). A *cis*-acting element in the 3′-UTR of the transcript enhances splicing of this mRNA (75). An example of destabilization of pre-mRNA in the nucleus is observed with peptidylglycine $\alpha$-amidating monooxygenase mRNA accumulation in the anterior pituitary. Analysis of the nuclear RNA showed that decreased peptidylglycine $\alpha$-amidating monooxygenase expression after 17$\beta$-estradiol treatment was primarily due to intranuclear destabilization of the primary transcript (76). Together, these data are consistent with the presence of a nuclear pathway for RNA degradation.

In contrast to examples that only involve posttranscriptional regulation, nutritional regulation of spot 14 occurs by large changes in the rate of transcription of this gene (60). However, along with the large transcriptional changes, dietary carbohydrate, and insulin result in accumulation of splicing intermediates for spot 14 pre-mRNA and an increased ratio of mature to pre-mRNA (61, 62). Thus, nuclear posttranscriptional regulation is not exclusive to genes that lack transcriptional regulation. We have confirmed these findings and found that, like G6PD, the amount of spot 14 spliced RNA was increased during

refeeding (Fig. 7). Regulation of this gene by both transcriptional and posttranscriptional mechanisms would result in a more rapid response to changing nutritional conditions. Further, these results suggest that regulation of the efficiency of splicing may be involved in the regulation of other lipogenic enzymes; it simply has not been studied due to the large transcriptional regulation of these genes (5). It remains to be determined if the fine details of this nuclear posttranscriptional regulation are the same across the genes known to exhibit this form of regulation.

Splicing is known to be regulatory in a number of physiological situations. The mechanisms involved in nuclear degradation remain to be determined. Two pathways have been identified that could regulate nuclear pre-mRNA levels. One pathway has been observed when splicing of a transgene was blocked by mutation, *e.g.* inhibition of splicing of a $\beta$-globin transgene resulted in the failure to further process the mRNA and it was degraded within the nucleus (37). Nuclear degradation can also involve the presence of a premature termination codon in the mRNA (77, 78). Apart from genetic mutations, a premature termination codon could arise due to the prolonged presence of an intron in the pre-mRNA. Distinguishing between these possibilities in the regulation of G6PD expression is the subject of future experiments in the laboratory.

*Acknowledgment*—We are gratefully acknowledge Dr. Michael J. Getz (deceased, Mayo Clinic, Rochester, MN) and Dr. Paula Elder in his laboratory for providing the mouse $\beta$-actin intronic sequence and Dr. Richard Planells (INSERM, Marseille, France) for providing the mouse spot 14 intronic sequence. We thank Dr. Jeffrey Nickerson (University of Massachusetts, Worchester, MA) for the gift of B1C8 monoclonal antibody, Dr. Mike Miller and Samantha Gadd (of this institution) for providing the MCF7 breast adenocarcinoma cell line, and Huimin Tao in our laboratory for the preparation of primary rat hepatocytes. We thank Dr. James Davie, Ronald Berezney, and Jim Mahaney for helpful discussions; Dr. Marilyn Evans and Huimin Tao for critically reading the manuscript; and Dr. Michael Kashon (NIOSH, Centers for Disease Control, Morgantown, WV) for help with the statistical analysis.

REFERENCES

1. Glock, G. E., and McLean, P. (1954) *Biochem. J.* **56,** 171–175
2. Glock, G. E., and McLean, P. (1955) *Biochem. J.* **61,** 390–397
3. Tepperman, H. M., and Tepperman, J. (1964) *Am. J. Physiol.* **206,** 357–361
4. Rognstad, R., and Katz, J. (1979) *J. Biol. Chem.* **254,** 11969–11972
5. Hillgartner, F. B., Salati, L. M., and Goodridge, A. G. (1995) *Physiol. Rev.* **75,** 47–76
6. Blake, W. L., and Clarke, S. D. (1990) *J. Nutr.* **120,** 1727–1729
7. Paulauskis, J. D., and Sul, H. S. (1989) *J. Biol. Chem.* **264,** 574–577
8. Stapleton, S. R., Mitchell, D. A., Salati, L. M., and Goodridge, A. G. (1990) *J. Biol. Chem.* **265,** 18442–18446
9. Hillgartner, F. B., Charron, T., and Chesnut, K. A. (1996) *Biochem. J.* **319,** 263–268
10. Katsurada, A., Iritani, N., Fukuda, H., Matsumura, Y., Nishimoto, N., Noguchi, T., and Tanaka, T. (1990) *Eur. J. Biochem.* **190,** 435–441
11. Ntambi, J. M. (1992) *J. Biol. Chem.* **267,** 10925–10930
12. Kim, K. S., Park, S. W., and Kim, Y. S. (1992) *Biochem. Biophys. Res. Commun.* **189,** 264–271
13. Dozin, B., Rall, J. E., and Nikodem, V. M. (1986) *Proc. Natl. Acad. Sci. U. S. A.* **83,** 4705–4709
14. Gonzalez, C. I., and Martin, C. E. (1996) *J. Biol. Chem.* **271,** 25801–25809
15. Sessler, A. M., Kaur, N., Palta, J. P., and Ntambi, J. M. (1996) *J. Biol. Chem.* **271,** 29854–29858
16. Berdanier, C. D., and Shubeck, D. (1979) *J. Nutr.* **109,** 1766–1771
17. Prostko, C. R., Fritz, R. S., and Kletzien, R. F. (1989) *Biochem. J.* **258,** 295–299
18. Gozukara, E. M., Frolich, M., and Holten, D. (1972) *Biochim. Biophys. Acta* **286,** 155–163
19. Watanabe, A., and Taketa, K. (1973) *Arch. Biochem. Biophys.* **158,** 43–52
20. Winberry, L., and Holten, D. (1977) *J. Biol. Chem.* **252,** 7796–7801
21. Wolfe, R. G., and Holten, D. (1978) *J. Nutr.* **108,** 1708–1717
22. Stabile, L. P., Hodge, D. L., Klautky, S. A., and Salati, L. M. (1996) *Arch. Biochem. Biophys.* **332,** 269–279
23. Hodge, D. L., and Salati, L. M. (1997) *Arch. Biochem. Biophys.* **348,** 303–312
24. Berezney, R., and Coffey, D. S. (1977) *J. Cell Biol.* **73,** 616–637
25. Berezney, R., and Coffey, D. S. (1974) *Biochem. Biophys. Res. Commun.* **60,** 1410–1417
26. Nickerson, J. A., Blencowe, B. J., and Penman, S. (1995) *Int. Rev. Cytol.* 67–123
27. Blencowe, B. J., Nickerson, J. A., Issner, R., Penman, S., and Sharp, P. A. (1994) *J. Cell Biol.* **127,** 593–607
28. Ciejek, E. M., Nordstrom, J. L., Tsai, M. J., and O'Malley, B. W. (1982) *Biochemistry* **21,** 4945–4953
29. Misteli, T., and Spector, D. L. (1999) *Mol. Cell* **3,** 697–705
30. Mortillaro, M. J., Blencowe, B. J., Wei, X., Nakayasu, H., Du, L., Warren, S. L., Sharp, P. A., and Berezney, R. (1996) *Proc. Natl. Acad. Sci. U. S. A.* **93,** 8253–8257
31. Nakayasu, H., and Berezney, R. (1991) *Proc. Natl. Acad. Sci. U. S. A.* **88,** 10312–10316
32. Schroder, H. C., Trolltsch, D., Friese, U., Bachmann, M., and Muller, W. E. (1987) *J. Biol. Chem.* **262,** 8917–8925
33. Zeitlin, S., Parent, A., Silverstein, S., and Efstratiadis, A. (1987) *Mol. Cell. Biol.* **7,** 111–1120
34. Sun, J. M., Chen, H. Y., and Davie, J. R. (1994) *J. Cell. Biochem.* **55,** 252–263
35. Hirose, Y., and Manley, J. L. (2000) *Genes Dev.* **14,** 1415–1429
36. McCracken, S., Fong, N., Yankulov, K., Ballantyne, S., Pan, G., Greenblatt, J., Patterson, S. D., Wickens, M., and Bentley, D. L. (1997) *Nature* **385,** 357–361
37. Custodio, N., Carmo-Fonseca, M., Geraghty, F., Pereira, H. S., Grosveld, F., and Antoniou, M. (1999) *EMBO J.* **18,** 2855–2866
38. Stabile, L. P., Klautky, S. A., Minor, S. M., and Salati, L. M. (1998) *J. Lipid Res.* **39,** 1951–1963
39. Leppard, K. N., and Shenk, T. (1989) *EMBO J.* **8,** 2329–2336
40. Chomczynski, P., and Sacchi, N. (1987) *Anal. Biochem.* **162,** 156–159
41. Laemmli, U. K. (1970) *Nature* **227,** 680–685
42. Wan, K. M., Nickerson, J. A., Krockmalnic, G., and Penman, S. (1994) *Proc. Natl. Acad. Sci. U. S. A.* **91,** 594–598
43. Grillasca, J. P., Gastaldi, M., Khiri, H., Dace, A., Peyrol, N., Reynier, P., Torresani, J., and Planells, R. (1997) *FEBS Lett.* **401,** 38–42
44. Elder, P. K., French, C. L., Subramaniam, M., Schmidt, L. J., and Getz, M. J. (1988) *Mol. Cell. Biol.* **8,** 480–485
45. Porter, D., and Curthoys, N. P. (1997) *Anal. Biochem.* **247,** 279–286
46. Zollo, M., D'Urso, M., Schlessinger, D., and Chen, E. Y. (1993) *DNA Seq.* **3,** 319–322
47. Carrazana, E. J., Pasieka, K. B., and Majzoub, J. A. (1988) *Mol. Cell. Biol.* **8,** 2267–2274
48. Fey, E. G., Krochmalnic, G., and Penman, S. (1986) *J. Cell Biol.* **102,** 1654–1665
49. Kallajoki, M., Weber, K., and Osborn, M. (1991) *EMBO J.* **10,** 3351–3362
50. Tousson, A., Zeng, C., Brinkley, B. R., and Valdivia, M. M. (1991) *J. Cell Biol.* **112,** 427–440
51. Maekawa, T., Leslie, R., and Kuriyama, R. (1991) *Eur. J. Cell Biol.* **54,** 255–267
52. Zeng, C., He, D., Berget, S. M., and Brinkley, B. R. (1994) *Proc. Natl. Acad. Sci. U. S. A.* **91,** 1505–1509
53. Zeng, C., He, D., and Brinkley, B. R. (1994) *Cell Motil. Cytoskel.* **29,** 167–176
54. Tang, T. K., Tang, C. J., Chen, Y. L., and Wu, C. W. (1993) *J. Cell Sci.* **104,** 249–260
55. Tang, T. K., Tang, C. J., Chao, Y. J., and Wu, C. W. (1994) *J. Cell Sci.* **107,** 1389–1402
56. Compton, D. A., Szilak, I., and Cleveland, D. W. (1992) *J. Cell Biol.* **116,** 1395–1408
57. Eldridge, A. G., Li, Y., Sharp, P. A., and Blencowe, B. J. (1999) *Proc. Natl. Acad. Sci. U. S. A.* **96,** 6125–6130
58. Blencowe, B. J., Issner, R., Nickerson, J. A., and Sharp, P. A. (1998) *Genes Dev.* **12,** 996–1009
59. Jump, D. B., Clarke, S. D., MacDougald, O., and Thelen, A. (1993) *Proc. Natl. Acad. Sci. U. S. A.* **90,** 8454–8458
60. Jump, D. B., Bell, A., and Santiago, V. (1990) *J. Biol. Chem.* **265,** 3474–3478
61. Burmeister, L. A., and Mariash, C. N. (1991) *J. Biol. Chem.* **266,** 22905–22911
62. Walker, J. D., Burmeister, L. A., Mariash, A., Bosman, J. F., Harmon, J., and Mariash, C. N. (1996) *Endocrinology* **137,** 2293–2299
63. Hamblin, P. S., Ozawa, Y., Jefferds, A., and Mariash, C. N. (1989) *J. Biol. Chem.* **264,** 21646–21651
64. Liaw, C. W., and Towle, H. C. (1984) *J. Biol. Chem.* **259,** 7253–7260
65. Jump, D. B., Clarke, S. D., Thelen, A., and Liimatta, M. (1994) *J. Lipid Res.* **35,** 1076–1084
66. Goethe, R., and Phi-van, L. (1998) *J. Immunol.* **160,** 4970–4978
67. Murphy, D., Pardy, K., Seah, V., and Carter, D. (1992) *Mol. Cell. Biol.* **12,** 2624–2632
68. Neugebauer, K. M., and Roth, M. B. (1997) *Genes Dev.* **11,** 3279–3285
69. Antoniou, M., Geraghty, F., Hurst, J., and Grosveld, F. (1998) *Nucleic Acids Res.* **26,** 721–729
70. Pandolfi, P. P., Sonati, F., Rivi, R., Mason, P., Grosveld, F., and Luzzatto, L. (1995) *EMBO J.* **14,** 5209–5215
71. Ehretsmann, C. P., Chandler, L. A., and Bourgeois, S. (1995) *Mol. Cell. Endocrinol.* **110,** 185–194
72. Kiledjian, M., and Kadesch, T. (1991) *J. Biol. Chem.* **266,** 4207–4213
73. Zhou, H., Manji, S. S., Findlay, D. M., Martin, T. J., Heath, J. K., and Ng, K. W. (1994) *J. Biol. Chem.* **269,** 22433–22439
74. Gerez, L., Arad, G., Efrat, S., Ketzinel, M., and Kaempfer, R. (1995) *J. Biol. Chem.* **270,** 19569–19575
75. Osman, F., Jarrous, N., Ben-Asouli, Y., and Kaempfer, R. (1999) *Genes Dev.* **13,** 3280–3293
76. el Meskini, R., Delfino, C., Boudouresque, F., Hery, M., Oliver, C., and Ouafik, L. (1997) *Endocrinology* **138,** 379–388
77. Li, S., Leonard, D., and Wilkinson, M. F. (1997) *J. Exp. Med.* **185,** 985–992
78. Zhang, J., and Maquat, L. E. (1996) *RNA* **2,** 235–243